Involvement of the Tyro3 receptor and its intracellular partner Fyn signaling in Schwann cell myelination

Yuki Miyamoto[a], Tomohiro Torii[a], Shuji Takada[b], Nobuhiko Ohno[c], Yurika Saitoh[c], Kazuaki Nakamura[a], Akihito Ito[d], Toru Ogata[e], Nobuo Terada[f], Akito Tanoue[a], and Junji Yamauchi[a,g]

[a]Department of Pharmacology and [b]Department of Systems BioMedicine, National Research Institute for Child Health and Development, Setagaya, Tokyo 157-8535, Japan; [c]Interdisciplinary Graduate School of Medicine and Engineering, University of Yamanashi, Chuo, Yamanashi 409-3898, Japan; [d]Research Center, Nissei Bilis, Koga, Shiga 528-0052, Japan; [e]Department of Rehabilitation for the Movement Functions, National Rehabilitation Center for Persons with Disabilities Research Institute, Tokorozawa, Saitama 359-8555, Japan; [f]Graduate School of Medicine, Shinshu University, Matsumoto, Nagano 390-8621, Japan; [g]Graduate School of Medical and Dental Sciences, Tokyo Medical and Dental University, Bunkyo, Tokyo 113-8510, Japan

ABSTRACT **During early development of the peripheral nervous system, Schwann cell precursors proliferate, migrate, and differentiate into premyelinating Schwann cells. After birth, Schwann cells envelop neuronal axons with myelin sheaths. Although some molecular mechanisms underlying myelination by Schwann cells have been identified, the whole picture remains unclear. Here we show that signaling through Tyro3 receptor tyrosine kinase and its binding partner, Fyn nonreceptor cytoplasmic tyrosine kinase, is involved in myelination by Schwann cells. Impaired formation of myelin segments is observed in Schwann cell neuronal cultures established from Tyro3-knockout mouse dorsal root ganglia (DRG). Indeed, Tyro3-knockout mice exhibit reduced myelin thickness. By affinity chromatography, Fyn was identified as the binding partner of the Tyro3 intracellular domain, and activity of Fyn is downregulated in Tyro3-knockout mice, suggesting that Tyro3, acting through Fyn, regulates myelination. Ablating Fyn in mice results in reduced myelin thickness. Decreased myelin formation is observed in cultures established from Fyn-knockout mouse DRG. Furthermore, decreased kinase activity levels and altered expression of myelination-associated transcription factors are observed in these knockout mice. These results suggest the involvement of Tyro3 receptor and its binding partner Fyn in Schwann cell myelination. This constitutes a newly recognized receptor-linked signaling mechanism that can control Schwann cell myelination.**

Monitoring Editor
Jonathan Chernoff
Fox Chase Cancer Center

Received: May 29, 2014
Revised: Jul 21, 2015
Accepted: Jul 23, 2015

INTRODUCTION

During development of the peripheral nervous system (PNS), Schwann lineage cells, myelin-forming glial cells unique to the PNS, migrate along neuronal axons to their final destinations, where they eventually wrap around individual axons to form the myelin sheath. The myelin sheath is a morphologically differentiated Schwann cell plasma membrane that insulates axons and markedly increases the nerve conduction velocity (Bunge, 1993). Over time, myelin sheaths can grow to be >100 times larger than the collective surface area of premyelinating Schwann cell plasma membranes. Growth factors, such as neuregulin-1 (NRG1), and adhesion molecule ligands, including various integrins, which are primarily produced by peripheral neurons, bind to their cognate receptors on Schwann cells, and their receptor activity regulates myelination (Nave and Salzer, 2006; Mirsky *et al.*, 2008; Taveggia *et al.*, 2010; Pereira *et al.*, 2012; Miyamoto and Yamauchi, 2014).

This article was published online ahead of print in MBoC in Press (http://www.molbiolcell.org/cgi/doi/10.1091/mbc.E14-05-1020) on July 29, 2015.

Address correspondence to: Junji Yamauchi (yamauchi-j@ncchd.go.jp).

Abbreviations used: DAPI, 4′,6-diamidino-2-phenylindole; GAP43, growth-associated protein 43; GFAP, glial fibrillary acidic protein; IGF-1, insulin-like growth factor 1; MBP, myelin basic protein; MPZ, myelin protein zero; NF68, 68-kDa neurofilament subunit; PDGF, platelet-derived growth factor; PNS, peripheral nervous system; TAM, Tyro3, Axl, and Mertk.

Tyro3 is a receptor tyrosine kinase member belonging to the Tyro3, Axl, and Mertk (TAM) receptor family. It participates in multiple cellular functions, including cell growth and differentiation (Lemke and Rothlin, 2010). Tyro3 is has the same domain structure as the other two members: two immunoglobulin-like domains, two fibronectin type II–like modules, a single transmembrane region, and an intracellular tyrosine kinase domain. Protein S and growth arrest-specific 6 (Gas6) bind to all three TAM receptors. Protein S is a protein abundant in serum, whereas Gas6 is an S-like protein that is present in tissues (Stitt *et al.*, 1995; Godowski *et al.*, 1995). In the PNS, Gas6 is specifically produced in neurons. Gas6 acts as a potent mitogen for primary Schwann cells in humans (Li *et al.*, 1996). The question of whether Tyro3 signaling is also involved in myelination remains to be resolved.

Fyn belongs to the Src family of tyrosine kinases of the nonreceptor type in cells (Hunter, 2009). Like other Src family kinases, Fyn is localized in the intracellular surface of the plasma membrane and transduces various extracellular signals intracellularly through the plasma membrane. Here we show that Tyro3 regulates Schwann cell myelination and that Fyn mediates Tyro3 signaling in Schwann cells. Impaired myelin formation is observed in Schwann cell neuronal cultures established from Tyro3-knockout mouse dorsal root ganglia (DRG). Tyro3-knockout mice exhibit reduced myelin thickness during development. Of importance, the intracellular domain of Tyro3 interacts with Fyn, and Tyro3 regulates Fyn activity. Similar to the phenotypes of Tyro3-knockout mice, Fyn- knockout mice exhibit reduced myelin thickness. Decreased myelin formation is also seen in cultures established from Fyn-knockout mouse DRG. Thus we can add Tyro3 to the list of Schwann cell receptors controlling myelination and identify Fyn as one of the intracellular signal transducers, thus defining a previously unknown receptor-mediated signaling mechanism underlying myelination.

RESULTS

Tyro3 is involved in Schwann cell myelination

To investigate whether Tyro3 is involved in Schwann cell myelination, we established Schwann cell neuronal cultures from Tyro3$^{-/-}$-mouse DRGs. Cultures from Tyro3$^{-/-}$ mice exhibited impaired formation of myelin segments positive for the myelin marker myelin basic protein (MBP) compared with those from littermate controls (Figure 1, A and B). These results are consistent with data showing decreased expression levels of another myelin marker, myelin protein zero (MPZ; also called P0), in Tyro3$^{-/-}$ sciatic nerve extracts (Figure 1C), suggesting that Tyro3 is involved in Schwann cell myelination. Next, to confirm that Tyro3 is expressed in Schwann cells, we isolated primary Schwann cells and DRG neurons from wild-type mice and performed immunoblotting using an anti-Tyro3 antibody. Tyro3 was specifically expressed in S100β-expressing Schwann cells but not in 68-kDa neurofilament subunit (NF68)- and growth-associated protein 43 (GAP43)-expressing DRG neurons (Figure 1D), consistent with previous results (Li *et al.*, 1996). In addition, of the three known TAM receptor family members (Tyro3, Axl, and Mertk), Tyro3 was the primary transcript in Schwann cells (Figure 1E). Further, Tyro3 was not detected in βIII tubulin–positive neurons but only in the surrounding regions, which were immunostained with a Schwann cell marker, glial fibrillary acidic protein (GFAP), or S100β (Figure 1F). These results suggest that Tyro3 is expressed in Schwann cells.

We then performed a myelin ultrastructural analysis of the sciatic nerve during development. Electron microscopic analyses show that sciatic nerves from 3-d-old Tyro3$^{-/-}$ mice exhibited reduced myelin thickness compared with those from littermate controls (Figure 2A). This finding was evident from quantification of the average *g* ratio, which is the numerical ratio between the diameter of the axon and the outer diameter of the myelinated fiber in the nerve cross section (Figure 2, B and C; average $g = 0.82 \pm 0.081$ in Tyro3$^{-/-}$ mice vs. 0.74 ± 0.098 in controls). Similar results were obtained not only in 2-wk-old mice (Supplemental Figure S1, A–C; average $g = 0.69 \pm 0.048$ in Tyro3$^{-/-}$ mice vs. 0.66 ± 0.053 in controls), but also in 2-mo-old mice (Figure 2, D–F; average $g = 0.65 \pm 0.058$ in Tyro3$^{-/-}$ mice vs. 0.61 ± 0.056 in controls), revealing a reduction of myelin thickness, at least until 2 mo of age. On the other hand, because distribution of axon diameters was comparable in Tyro3$^{+/+}$ and Tyro3$^{-/-}$ mice, Tyro3 knockout is unlikely to affect axon thickness. Whereas cultures from Tyro3$^{-/-}$ mice exhibited impaired formation of myelin segments, actual in vivo Tyro3$^{-/-}$ mouse sciatic nerves exhibited less severe impairment. This may be due to differences in growth factors available in vitro and in vivo. Another possibility may be differences in extracellular materials in the in vitro and in vivo experimental conditions.

We also measured the length between sodium channel–accumulating nodes in transverse sections of 1-mo-old mouse. The internode length in Tyro3$^{-/-}$ mice was 560 ± 57 μm, compared to 580 ± 48 μm in Tyro3$^{+/+}$ mice (Supplemental Figure S2, A and B). The length in Tyro3$^{+/+}$ mice is similar to the established one (Novak *et al.*, 2011). Although the difference between knockout mice and the controls was not large, Tyro3 is involved in mediating the length of the internode. These results suggest that the thinner myelin thickness observed in knockout mice is associated with shorter internode. We next measured the nerve conduction velocity in sciatic nerves. The velocities in knockout mice and controls were 33 ± 3.1 and 33 ± 4.3 m/s, respectively (Supplemental Figure S2C). The presence or absence of the *tyro3* gene in nerves did not have an influence on nerve conduction velocity. Thus it appears that Tyro3 knockout causes delayed myelination but not hypomyelination or incomplete myelination with defective nerve conduction velocity.

Because the Tyro3 ligand Gas6 is regarded as a potent mitogen of primary Schwann cells in humans in vitro (Li *et al.*, 1996), we examined the effect of Tyro3 knockout on basic cell biological events such as growth and migration in mouse primary Schwann cells. Indeed, stimulation with Gas6 modestly increased cell number and NRG1, as the positive control, markedly did the number. In contrast, Tyro3$^{-/-}$ cells did not respond to Gas6 (Figure 3A, bar 12 vs. bar 9). The difference in Gas6 response may be due to differences between human and mouse species and/or experimental conditions, although Tyro3 participates in regulating proliferation in mouse Schwann cells. In addition, Gas6 modestly increased cell migration in vitro, but the effect was not seen in Tyro3$^{-/-}$ cells (Figure 3, B, bar 6, vs. C, bar 3).

Next we tested whether knockout of Tyro3 affects basic cell biological events in vivo. We immunostained 6-d-old sciatic nerve cross sections, which contain Schwann cells and axons of neurons, with an antibody against Ki67 antigen or active, cleaved caspase 3. Ki67 antigen–positive cells are proliferating cells, whereas cleaved caspase 3–positive cells show apoptotically dying cells. The number of Ki67 antigen-positive cells was comparable between Tyro3$^{+/+}$ and Tyro3$^{-/-}$ nerves (Supplemental Figure S3, A and B). Cleaved caspase 3–positive cells were hardly detected in both strains (Supplemental Figure S3, C and D), suggesting that knockout of Tyro3 seems unrelated to Schwann cell proliferation and apoptosis in vivo. In addition, the number of 4′,6-diamidino-2-phenylindole (DAPI)–stained cells within nerves was comparable between Tyro3$^{+/+}$ and Tyro3$^{-/-}$ nerves (Supplemental Figure S3E). Thus Tyro3 does not appear to affect cell migration along peripheral nerves in vivo, although the knockout might delay migration in embryonic stages.

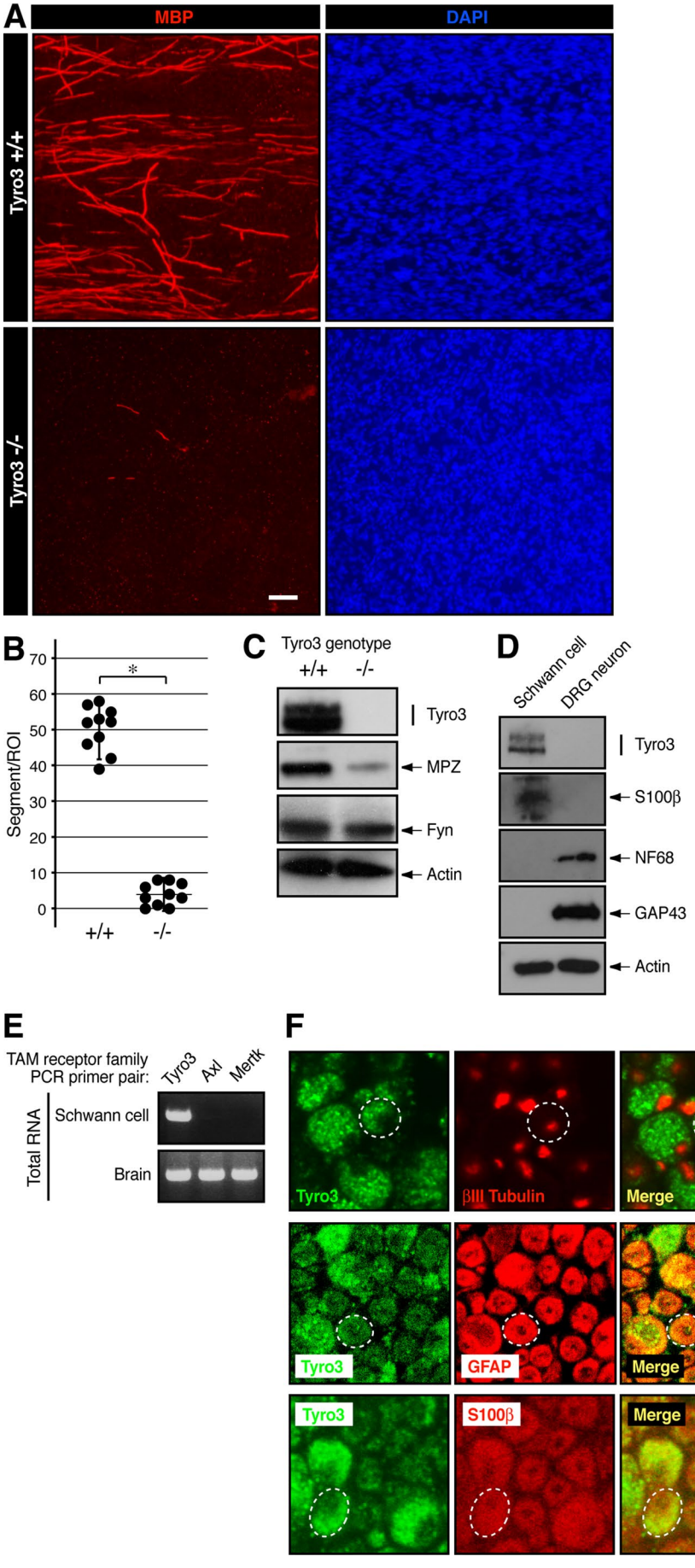

The intracellular tyrosine kinase domain of Tyro3 interacts with nonreceptor tyrosine kinase Fyn to regulate Fyn phosphorylation state

To explore which molecule intracellularly transduces signaling from Tyro3 and whether it regulates Schwann cell myelination, we expressed the myc-tagged intracellular tyrosine kinase domain of Tyro3 in the rat immortalized Schwann cell line RT4-D6P2T, lysed cells with buffer containing detergents, and collected protein complexes containing myc-tagged proteins. RT4-D6P2T cells exhibit Schwann cell–like spindle shape and express marker proteins, although they do not have the ability to produce a myelin sheath (Hai *et al.* 2002). Through in-gel digestion and mass spectrometric analysis of electrophoretically separated proteins (Miyamoto *et al.*, 2012; Yamauchi *et al.*, 2012), we identified a Tyro3-interacting, 60-kDa protein band as a mixture of Src family nonreceptor tyrosine kinase Fyn and lymphocyte-rich, lectin-like receptor Klrg1 (Figure 4A). It is known that in Cos-7 cells, Tyro3 is coimmunoprecipitated with an antibody against c-Src, which is the prototypic Src family kinase member (Toshima *et al.*, 1995). In addition, in the mouse brain, Fyn plays a key role in myelination by oligodendrocytes (Umemori *et al.*, 1994). We thus

FIGURE 1: Deletion of Tyro3 leads to decreased formation of myelin segments in cultures. (A, B) Schwann cell DRG neuronal cultures were established from Tyro3$^{+/+}$ and Tyro3$^{-/-}$ mouse embryonic DRGs and stained with an antibody against myelin marker protein MBP (red) or DAPI (blue). Scale bar, 20 μm. MBP-positive segments were counted in a 200-μm-square field (*$p < 0.01$; $n = 10$). (C) Tissue lysates from 6-d-old Tyro3$^{+/+}$ and Tyro3$^{-/-}$ mouse sciatic nerves were used for the respective immunoblottings. Expression levels of Tyro3, myelin marker protein MPZ, Fyn, and control actin. (D) Primary Schwann cells and neurons were isolated from wild-type mice, cultured, and used for the respective immunoblottings. Expression levels of Tyro3, Schwann cell marker protein S100β, neuronal cell marker proteins NF68 and GAP43, and control actin. (E) In Schwann cells, RT-PCR analysis detects the primary transcription of Tyro3. All TAM receptor members are detected in brain total RNA as the positive control. (F) Cross section of 6-d-old mouse sciatic nerve immunostained with antibodies for Tyro3 (green), and neuronal marker βIII tubulin (red), or Schwann cell marker S100β (red). A 7-d-old cross section was also immunostained with antibodies for Tyro3 (green) and Schwann cell marker GFAP (red). Dotted circle indicates a typical axon with Schwann cells. Scale bar, 5 μm.

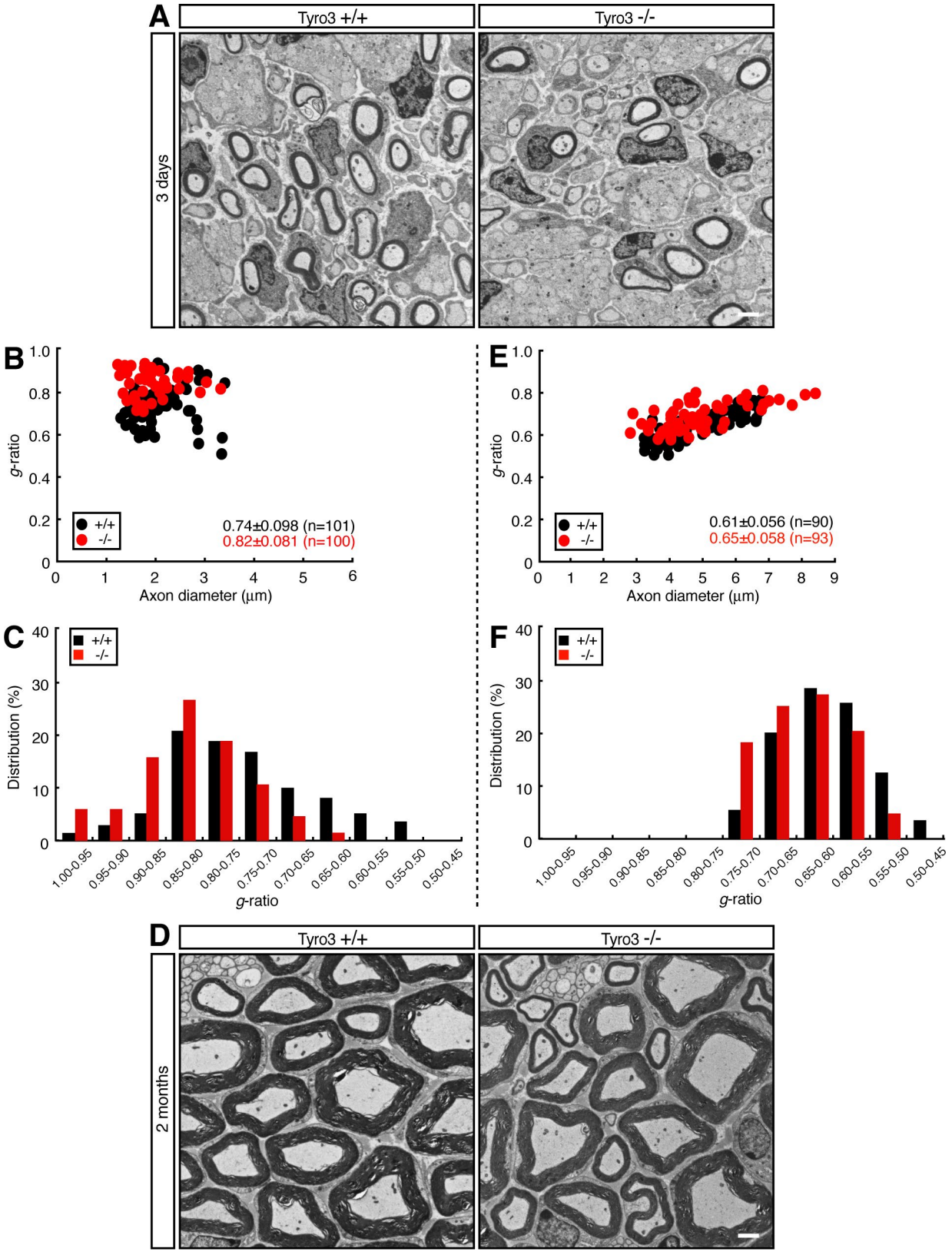

FIGURE 2: Deletion of Tyro3 leads to decreased myelin thickness in mice. (A) Electron microscopic photographs of 3-d-old Tyro3$^{+/+}$ and Tyro3$^{-/-}$ mouse sciatic nerves (n = 101 and 100, respectively). Scale bar, 1 μm. (B) The g ratio—the numerical ratio between the diameter of the axon and the outer diameter of the myelinated fiber—plotted vs. axon diameter. The average g ratio is also given. (C) The data from 3-d-old mice in the form of the relative distribution of the g ratio. (D) Electron microscopic photographs of 2-mo-old Tyro3$^{+/+}$ and Tyro3$^{-/-}$ mouse sciatic nerves (n = 90 and 93, respectively). Scale bar, 1 μm. (E) The g ratio vs. axon diameter for these mice. The average g ratio is also given. (F) The relative distribution of the g ratio for these mice.

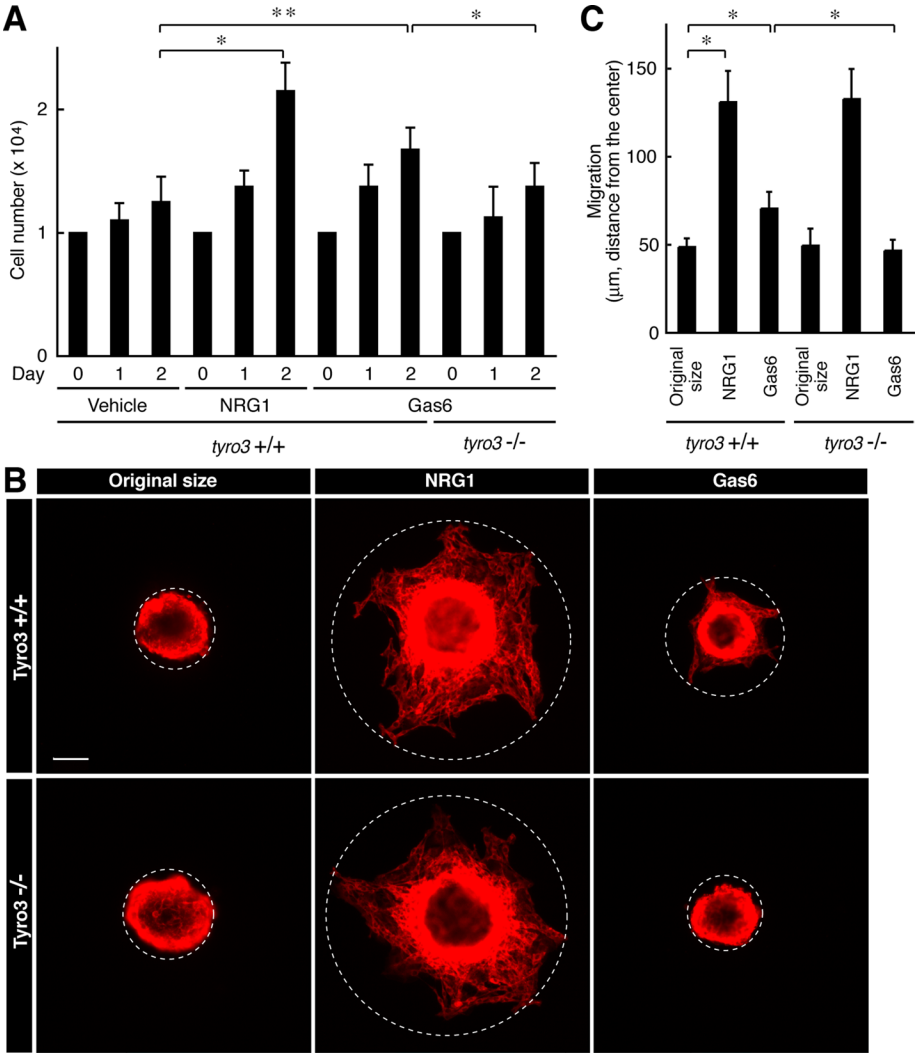

FIGURE 3: Deletion of Tyro3 inhibits Gas6-stimulated Schwann cell proliferation and migration. (A) Tyro3$^{+/+}$ or Tyro3$^{-/-}$ Schwann cells were cultured for 1 or 2 d in normal medium with or without 20 ng/ml Gas6 (*$p < 0.01$; **$p < 0.025$; $n = 4$). Treatment with 20 ng/ml NRG1 was used as the positive control. (B, C) Reaggregated Tyro3$^{+/+}$ or Tyro3$^{-/-}$ Schwann cells were allowed to migrate outward for 6 h in normal medium with or without 20 ng/ml Gas6 and stained with an antibody against S100β. Treatment with NRG1 was used as the positive control. The dotted circles indicate the maximum peripheries of Schwann cells migrating from the reaggregates. The distance furthest from the center was measured as the migrating distance (*$p < 0.01$; $n = 4$). Scale bar, 50 μm.

focused on Fyn and tried to determine whether Fyn is the intracellular signal transducer of Tyro3 in Schwann cells. In Tyro3$^{-/-}$-mouse sciatic nerves, immunoblotting showed that phosphorylation levels of the Fyn autophosphorylation site (Tyr-420) in the kinase activation loop (Hunter, 2009) were decreased. In contrast, phosphorylation of the C-terminal tyrosine residue (Tyr-531) by negative regulators such as Csk (Hunter, 2009) was increased in Tyro3$^{-/-}$ nerves (Figure 4B), indicating that Fyn can be regulated by Tyro3 in Schwann cells.

Fyn is involved in Schwann cell myelination

In Figure 4C, our hypothesis that Fyn is involved in Schwann cell myelination is supported by results that showed decreased expression levels of MPZ in Fyn$^{-/-}$ sciatic nerve extracts. Unlike the expression profile of Tyro3, Fyn was expressed in both Schwann cells and DRG neurons; however, the expression levels in Schwann cells were greater than those in neurons (Figure 4D). We thus examined the effects of Fyn knockout on DRG neurons. Expression levels of the neuronal markers and the activities of morphological regulators Rac1 and Cdc42 were comparable in Fyn$^{+/+}$ and Fyn$^{-/-}$ mice (Figure 4E; Arimura and Kaibuchi, 2007; Hall and Lalli, 2010), suggesting that Fyn knockout seems unlikely to affect neurons.

Next we established Schwann cell neuronal cultures from Fyn$^{-/-}$ mouse DRG. Cultures from Fyn$^{-/-}$ mice exhibited impaired formation of MBP-positive myelin segments compared with those from littermate controls (Figure 4, F and G). In electron microscopic analysis, 3-d-old Fyn$^{-/-}$ mice exhibited reduced myelin thickness compared with littermate controls (Figure 5, A–C; average $g = 0.77 \pm 0.059$ in Fyn$^{-/-}$ mice vs. 0.73 ± 0.063 in controls). Similar results were observed in 2-mo-old mice (Figure 5, D–F; average $g = 0.64 \pm 0.058$ in Fyn$^{-/-}$ mice vs. 0.62 ± 0.057 in controls), revealing a reduction of myelin thickness, as seen in Tyro3$^{-/-}$ mice. On the other hand, because distribution of axon diameters was comparable in Fyn$^{+/+}$ and Fyn$^{-/-}$ mice, Fyn knockout does not appear to affect axon thickness.

Thus, to investigate whether Fyn recovers Tyro3$^{-/-}$ thin myelin structure, we generated active Fyn transgenic mice. Transgenic mice were interbred with Tyro3$^{-/-}$ mice, and electron microscopic analysis in 2.5-d-old sciatic nerves was performed. In active Fyn transgenic Tyro3$^{-/-}$ mice, average g was 0.70 ± 0.055. In contrast, the value for Tyro3$^{-/-}$ mice was 0.81 ± 0.043 (Figure 6, A–C), suggesting that Fyn can rescue the Tyro3$^{-/-}$ thin-myelin phenotype. Expression of active Fyn in sciatic nerves was confirmed by immunoblotting (Figure 6D). It is thus believed that Tyro3 acts upstream of Fyn, at least in the initiation of myelination.

On the other hand, Fyn$^{-/-}$ Schwann cells failed to respond to Gas6-stimulated cell proliferation (Figure 7A) and migration (Figure 7, B and C) in vitro; however, the number of Ki67 antigen–positive cells was comparable between Fyn$^{+/+}$ and Fyn$^{-/-}$ nerves (Supplemental Figure S4, A and B). In addition, cleaved caspase 3–positive cells were barely detected in either stain (Supplemental Figure S4, C and D). Further, the number of DAPI-stained cells in nerve tissues was comparable between Tyro3$^{+/+}$ and Tyro3$^{-/-}$ mice (Supplemental Figure S4E), suggesting that Fyn knockout does not have an effect on Schwann cell growth and migration in vivo.

Effects of Tyro3 or Fyn knockout on Akt phosphorylation or myelination-associated transcription factor expression

Akt kinase plays a key role in myelination, and phosphorylation levels of Ser-473 in the kinase activation loop are associated with triggering myelination (Macklin, 2010; Krishnan, 2013). Because the phosphorylation levels reflect the progress of myelination, they are often used as one of the markers of myelination (Macklin, 2010;

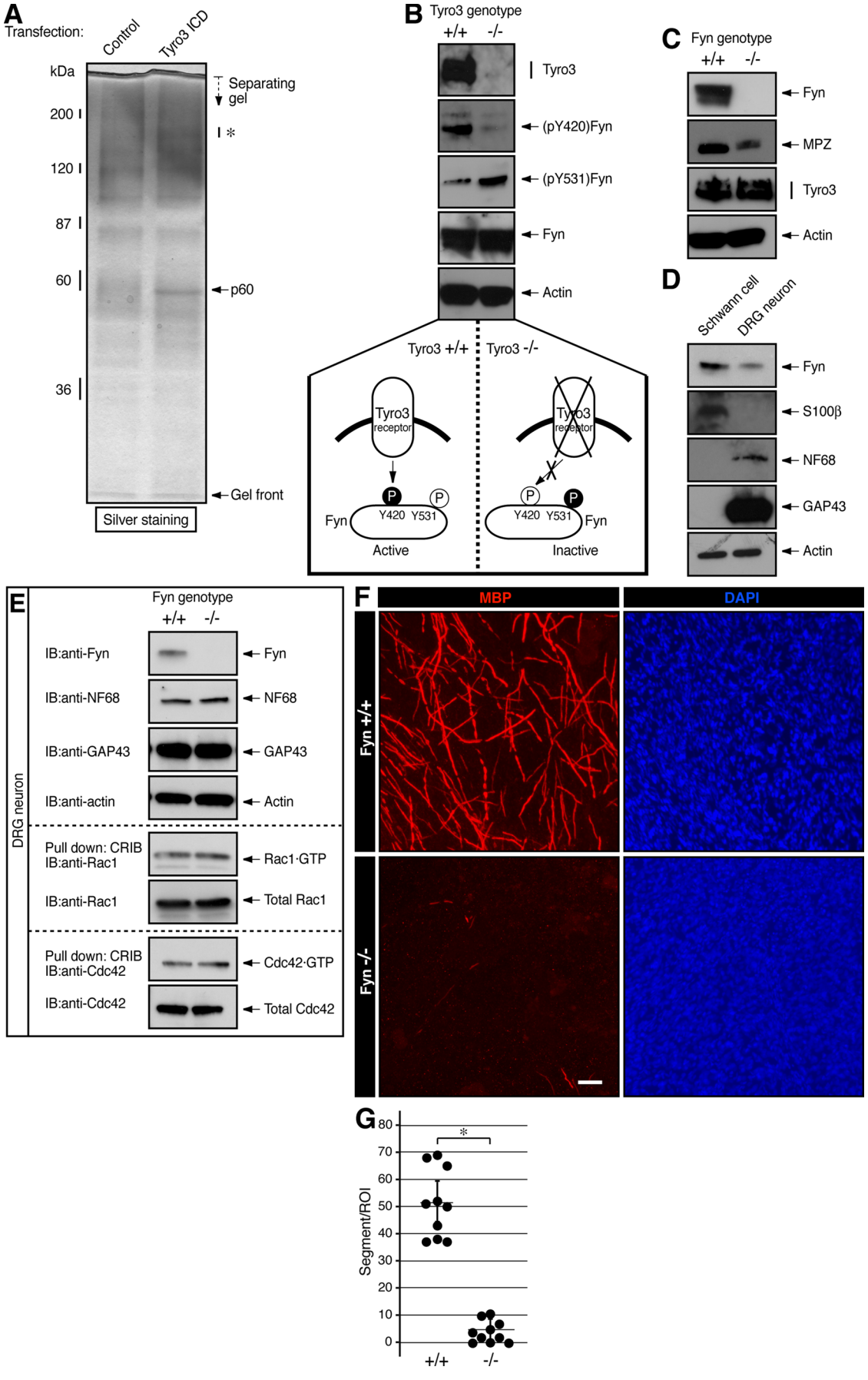
A
Transfection:
Control
Tyro3 ICD
kDa
200
120
87
60
36
Separating gel
*
p60
Gel front
Silver staining
B
Tyro3 genotype
+/+ -/-
Tyro3
(pY420)Fyn
(pY531)Fyn
Fyn
Actin
Tyro3 +/+
Tyro3 -/-
Tyro3 receptor
P
Y420 Y531
Fyn
Active
Inactive
C
Fyn genotype
+/+ -/-
Fyn
MPZ
Tyro3
Actin
D
Schwann cell
DRG neuron
Fyn
S100β
NF68
GAP43
Actin
E
Fyn genotype
+/+ -/-
DRG neuron
IB:anti-Fyn
Fyn
IB:anti-NF68
NF68
IB:anti-GAP43
GAP43
IB:anti-actin
Actin
Pull down: CRIB
IB:anti-Rac1
Rac1·GTP
IB:anti-Rac1
Total Rac1
Pull down: CRIB
IB:anti-Cdc42
Cdc42·GTP
IB:anti-Cdc42
Total Cdc42
F
MBP
DAPI
Fyn +/+
Fyn -/-
G
Segment/ROI
80
70
60
50
40
30
20
10
0
*
+/+
-/-

Krishnan, 2013). Neither Tyro3$^{-/-}$ nor Fyn$^{-/-}$ nerves showed increased phosphorylation at days 6 and 12 (Figure 8, A and B), although basal Akt phosphorylation levels were retained in knockout backgrounds. In contrast, Akt expression levels were comparable in wild-type and knockout mice. These results suggest delayed myelination in these knockout mice.

Changes in expression levels of two transcription factors, Oct6 (also called Scip) and Krox20 (also called Egr2), are essential for Schwann cell myelination (Nave and Salzer, 2006; Mirsky *et al.*, 2008). At the start of the myelination in particular, Oct6 is down-regulated and Krox20 is up-regulated (Nave and Salzer, 2006; Mirsky *et al.*, 2008). Thus Oct6 and Krox20 have also been used as myelination markers. It is believed that their expression is regulated by Akt kinase (Macklin, 2010; Krishnan, 2013). Expression levels of Oct6 in 1-d-old sciatic nerves were slightly decreased in both Tyro3$^{-/-}$ and Fyn$^{-/-}$ nerves (Figure 9, A and B). These results may suggest delayed myelination in knockout mice. In addition, expression levels of Krox20 were decreased in both Tyro3$^{-/-}$ and Fyn$^{-/-}$ nerves (Figure 9, C and D), consistent with the results from phosphorylation levels of Akt kinase. Expression levels of the control actin were comparable (Figure 9, E and F).

These results using possible myelination markers, Akt kinase, and transcription factors also support the notion that signaling through Tyro3 and Fyn is involved in Schwann cell myelination.

DISCUSSION

Among receptor tyrosine kinases, it is well established that the ErbB2 and ErbB3 heterodimer promotes myelination by Schwann cells (Lemke, 2001; Nave and Salzer, 2006; Newbern and Birchmeier, 2010). A neuronal type III alternative splicing variant of NRG1 is one of the major ligands to promote Schwann cell myelination. The type III ligand binds to the ErbB3 receptor on Schwann cells. ErbB3 has only a very low kinase activity, but ligand binding to ErbB3 up-regulates the intrinsic high ErbB2 kinase activity. The activated ErbB2 and ErbB3 heterodimer plays a key role in myelination. In other examples, insulin-like growth factor 1 (IGF-1) and platelet-derived growth factors (PDGFs) are also produced by peripheral neurons, and their respective receptor tyrosine kinases on Schwann cells modulate myelination (Ogata *et al.*, 2004). IGF-1 action on Schwann cells positively regulates myelination, whereas PDGFs negatively regulate it (Ogata *et al.*, 2004; Monje *et al.*, 2009). The neurotrophin-3 receptor tyrosine kinase (TrkC) is also expressed in Schwann cells and is involved in myelination, although TrkC has only an inhibitory effect on myelination (Chan *et al.*, 2001; Cosgaya *et al.*, 2002). In the present study, we identified Tyro3 as one of the receptor tyrosine kinases that can promote Schwann cell myelination.

It is clear that Tyro3 can regulate Schwann cell myelination processes, but the effects of the Tyro3 ligand Gas6 and that of Tyro3 itself are mild in our experiments. Tyro3 knockout does not cause hypomyelination or incomplete myelination with defective nerve conduction velocity. This may be due to the fact that Schwann cells have various types of interactions with neurons or extracellular matrixes that are also involved in regulation of Schwann cell morphological changes and myelination, compensating for the effect of Tyro3 deletion. For example, extracellular matrix laminin binding to integrins on Schwann cells plays a key role in Schwann cell adhesion, morphological changes, and myelination (Taveggia *et al.*, 2010; Pereira *et al.*, 2012). In addition, besides homophilic interaction between the typical cell adhesion molecules (cadherins), axonal Necl1 binding to Schwann cell Necl4 is known to regulate myelination processes (Spiegel *et al.*, 2007; Taveggia *et al.*, 2010; Pereira *et al.*, 2012). Another possible reason is that tyrosine kinase receptor signaling, as mentioned earlier, may act together with Tyro3 signaling to regulate Schwann cell myelination.

TAM receptors, such as Tyro3, are known to contribute to myelination by oligodendrocytes in the CNS (Binder *et al.*, 2008; Binder and Kilpatrick, 2009). Activation of Tyro3 regulates oligodendrocyte myelination during development, although the underlying mechanism is unclear (Binder *et al.*, 2008; Binder and Kilpatrick, 2009). Stimulation with Gas6 promotes oligodendrocyte myelination in vitro (Binder *et al.*, 2011). It increases the number of myelinated axons in the corpus callosum (Tsiperson *et al.*, 2010). It is likely that the TAM receptor plays a role in the regulation of myelination in both the PNS and the CNS.

The signaling pathway coupling TAM receptors to intracellular signal transducers is believed to be linked to two major downstream units: one pathway is toward the Janus kinase and the downstream signal transducer and activator of transcription unit, and the other is toward the phosphatidylinositol 3-kinase (PI3K) and the downstream Akt kinase unit. Although these two signaling pathways have been well studied in lymphocytes, the latter signaling unit is preserved in many types of cells other than lymphocytes, including Schwann cells (Lemke and Rothin, 2010; Taveggia *et al.*, 2010; Pereira *et al.*, 2012). In this study, we used Akt phosphorylation as a marker of the progress of Schwann cell myelination, but PI3K and Akt might also be involved in the Tyro3 signaling cascade. Indeed, in Tyro3$^{-/-}$-mouse sciatic nerves, Akt phosphorylation is down-regulated to the basal levels.

FIGURE 4: Tyro3 interacts with Fyn to regulate it in Schwann cells. (A) RT4-D6P2T cells were transfected with the control vector or myc-tagged Tyro3 intracellular tyrosine kinase domain (ICD). Coprecipitated proteins with Tyro3 ICD were collected with an anti-myc antibody and detected with silver staining. By mass spectrometric analysis, a Tyro3 ICD–interacting 60-kDa band (p60) was identified as a protein mixture of Fyn and Klrg1. In this experiment, the 150- to 180-kDa protein bands (indicated by an asterisk) were not identified. (B) Tissue lysates from Tyro3$^{+/+}$ or Tyro3$^{-/-}$ sciatic nerves were used for the respective immunoblottings. Phosphorylation levels of (pY420)Fyn and (pY531)Fyn in Fyn immunoprecipitates, as well as expression levels of Tyro3, Fyn, and control actin. Y420 phosphorylation in the kinase activation loop stimulates the activity of Fyn, whereas Y531 phosphorylation near the C-terminal position down-regulates Fyn (bottom schematic diagrams). (C) Tissue lysates from Fyn$^{+/+}$ or Fyn$^{-/-}$ sciatic nerves were used for the respective immunoblottings. Expression levels of Fyn, MPZ, Tyro3, and control actin. (D) Expression levels of Fyn, S100β, NF68, and GAP43, and control actin in Schwann cells and DRG neurons, (E) Cell lysates from Fyn$^{+/+}$ or Fyn$^{-/-}$ DRG neurons were used for the respective immunoblottings (Fyn, NF68, GAP43, control actin, and Rho GTPases Rac1 and Cdc42). They were also used for an affinity precipitation assay to detect with active, GTP-bound Rac1 or Cdc42, which are essential for forming neuronal structures. (F, G) Fyn$^{+/+}$-or Fyn$^{-/-}$-mouse Schwann cell DRG neuronal cultures were established from mouse embryonic DRG and stained with an antibody against MBP (red) or DAPI (blue). Scale bar, 20 μm. MBP-positive segments were counted in a 200-μm-square field (*$p < 0.01$; $n = 10$).

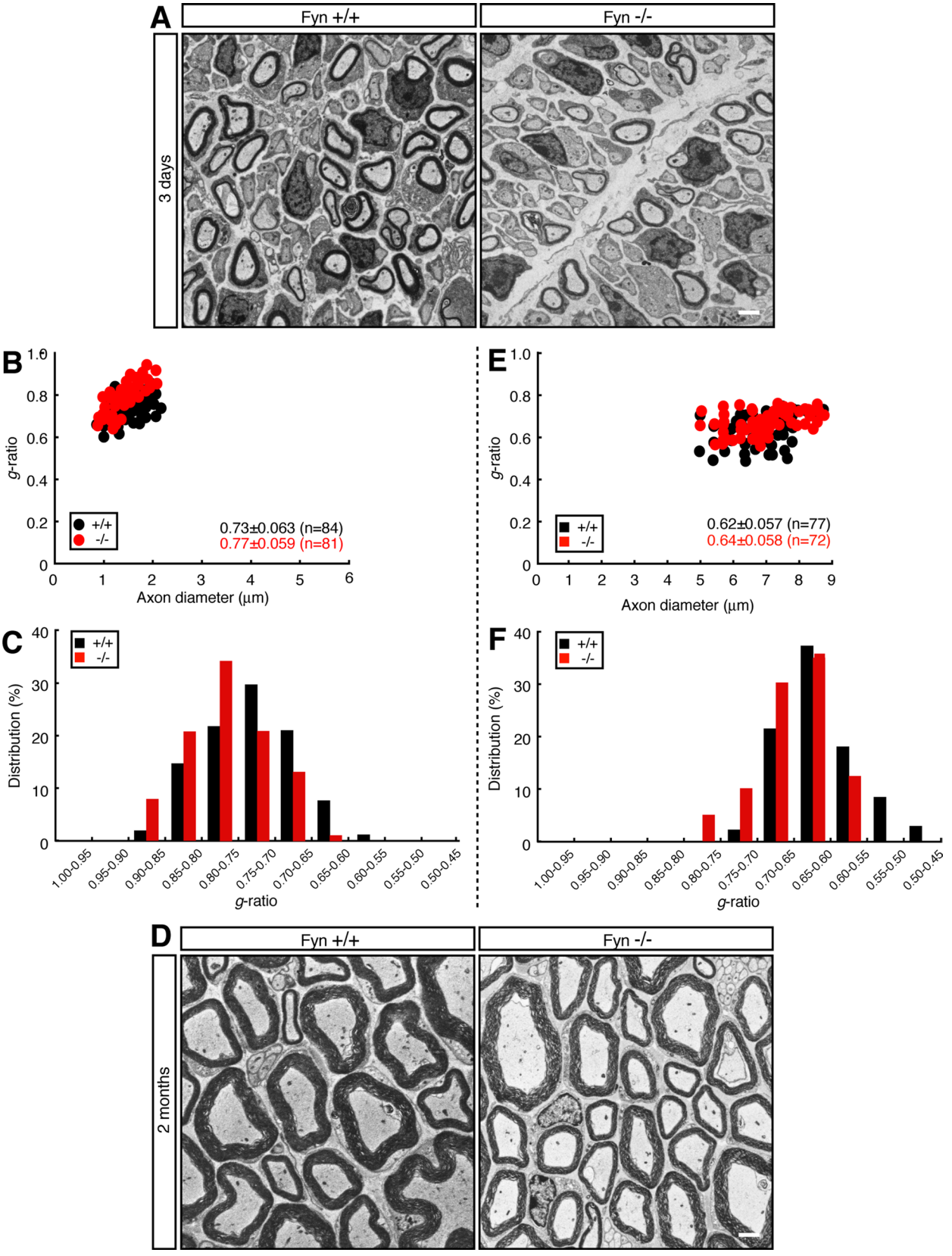

FIGURE 5: Electron microscopic analyses of sciatic nerves of Fyn-knockout mouse. (A) Electron microscopic photographs of 3-d-old $Fyn^{+/+}$ and $Fyn^{-/-}$ mouse sciatic nerves ($n = 84$ and 81, respectively). Scale bar, 1 μm. (B) The *g* ratio vs. axon diameter. The average *g* ratio is also given. (C) The relative distributions of the *g* ratio. (D) Electron microscopic photographs of 2-mo-old $Fyn^{+/+}$ and $Fyn^{-/-}$ mouse sciatic nerves ($n = 77$ and 72, respectively). Scale bar, 1 μm. (E) The *g* ratio vs. axon diameter for these mice. The average *g* ratio is also given. (F) The relative distribution of the *g* ratio for these mice.

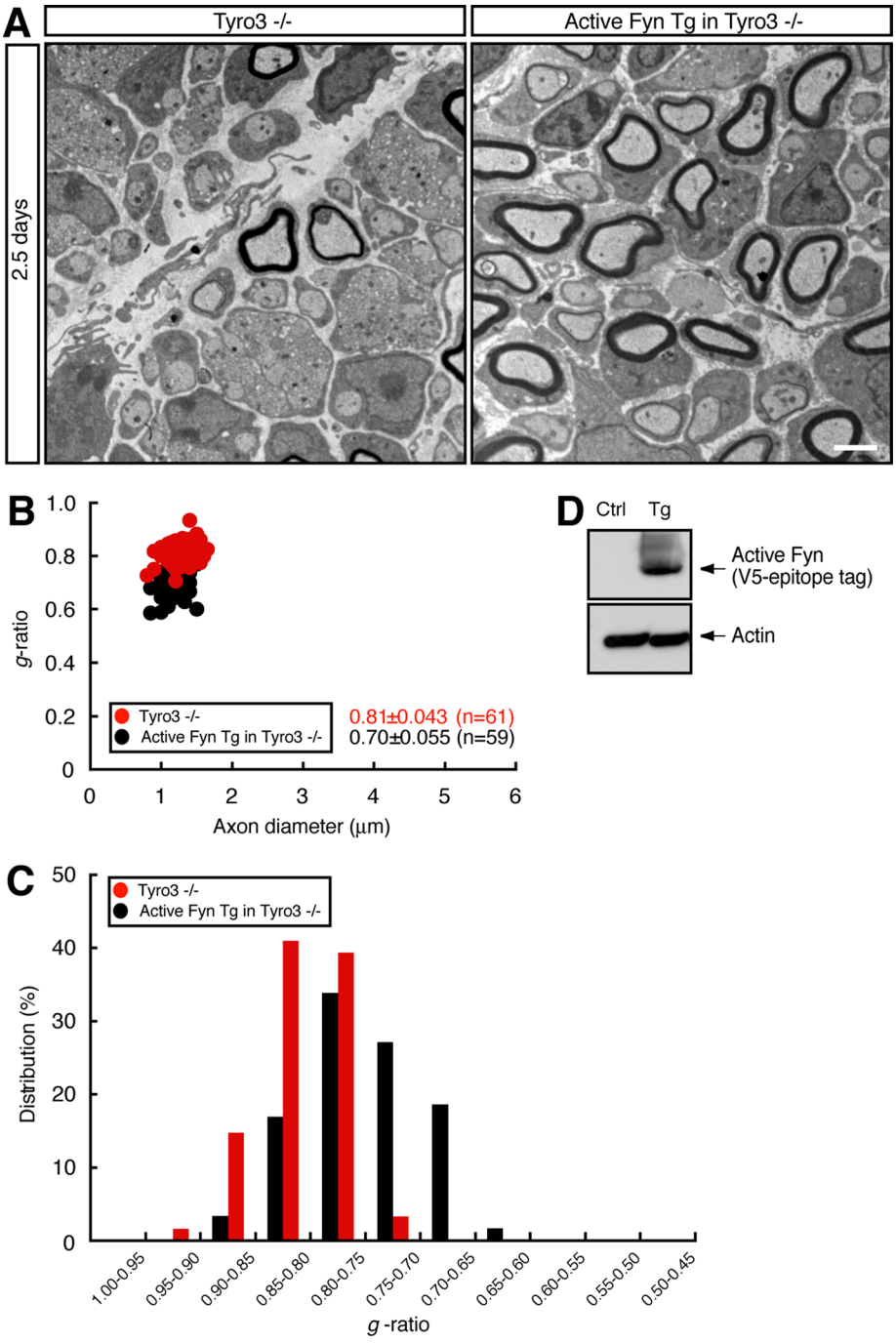

FIGURE 6: Interbreeding of Tyro3-knockout mice with Fyn transgenic mice can rescue the Tyro3- knockout mouse thin myelin structure. (A) Electron microscopic photographs of 2.5-d-old mouse sciatic nerves for Tyro3$^{-/-}$ mice and active Fyn transgenic (Tg) Tyro3$^{-/-}$ mice ($n = 61$ and 59, respectively). Scale bar, 1 μm. (B) The *g* ratio vs. axon diameter. The average *g* ratio is also given. (C) The relative distribution of the *g* ratio. (D) Sciatic nerve extracts from active Fyn transgenic (Tg) and control (Ctrl) mice immunoblotted with an antibody for V5-epitope tag or actin.

In Fyn$^{-/-}$ nerves, Akt phosphorylation is also decreased, suggesting that Tyro3 and Fyn can act upstream of Akt. Because nonreceptor tyrosine kinases, such as Fyn, generally have the ability to stimulate PI3K activity (Fritsch and Downward, 2013), Tyro3 receptor and the partner Fyn may be directly linked to PI3K and Akt in Schwann cells. It is believed that the PI3K and Akt unit regulates expression levels of the myelination-associated transcription factors Oct6 and Krox20 (Macklin, 2010; Krishnan, 2013). Thus it is possible that the Tyro3/Fyn/PI3K/Akt cascade in this study may exist in Schwann cells and regulate expression of these transcription factors to mediate Schwann cell myelination.

It is likely that in Schwann cells, Src family kinases, including c-Src, Lck, Fyn, and Lyn, cooperatively or independently promote myelination processes through their respective specific signaling pathways. c-Src is specifically localized in the Schmidt–Lanterman incisure, which is a specific feature of myelinated nerve fibers in the PNS, and forms a complex with membrane protein palmitoylated 6 and a cytoskeletal protein 4.1G possibly to mediate a localized signal (Terada *et al.*, 2013). Lck intracellularly mediates signals from cell adhesion molecules such as integrins to promote myelination in vivo (Ness *et al.*, 2013). Hossain *et al.* (2010) showed that Fyn and Lyn participate in increasing the number of myelinated axons in vitro. In vivo, Fyn couples signals from ErbB2/3 and IGF1 receptors to Arf6 guanine-nucleotide exchange factor cytohesin-1, which activates Arf6, a small GTPase family member. Fyn directly binds, phosphorylates, and activates cytohesin-1. Fyn results in promoting myelination, especially the initiating events (Yamauchi *et al.*, 2012; Torii *et al.*, 2013). It is conceivable that Fyn, acting downstream of Tyro3, may activate Arf6 to promote myelination.

On the other hand, in the CNS, Fyn plays a more critical role in myelination by oligodendrocytes (Umemori *et al.*, 1994; Sperber *et al.*, 2001). In oligodendrocyte differentiation and myelination, Fyn targets include the cytoskeletal proteins (tau and tubulin) and their upstream regulators, Rho-family small GTPase-activating proteins (p190RhoGAP and p250RhoGAP; Wolf *et al.*, 2001; Klein *et al.*, 2002; Taniguchi *et al.*, 2003). Because these proteins are widely distributed in neuronal tissues and mediate Rho-family small GTPase-regulated morphological changes, they may act downstream of Fyn in Schwann cells and be involved in myelination together with the Arf family.

In this study, for the first time we show that Tyro3 receptor is involved in myelination by Schwann cells. Tyro3 receptor interacts with Fyn nonreceptor tyrosine kinase to promote myelination. Further studies will allow us to clarify the detailed mechanism by which signaling through Tyro3 and Fyn regulates Schwann cell myelination. In addition, studies in this area may allow us to understand whether this mechanism is possibly conserved in one underlying myelination process by oligodendrocytes. Such studies on the mechanisms concerning myelination may help us to elucidate a paradigm for remyelination and nerve

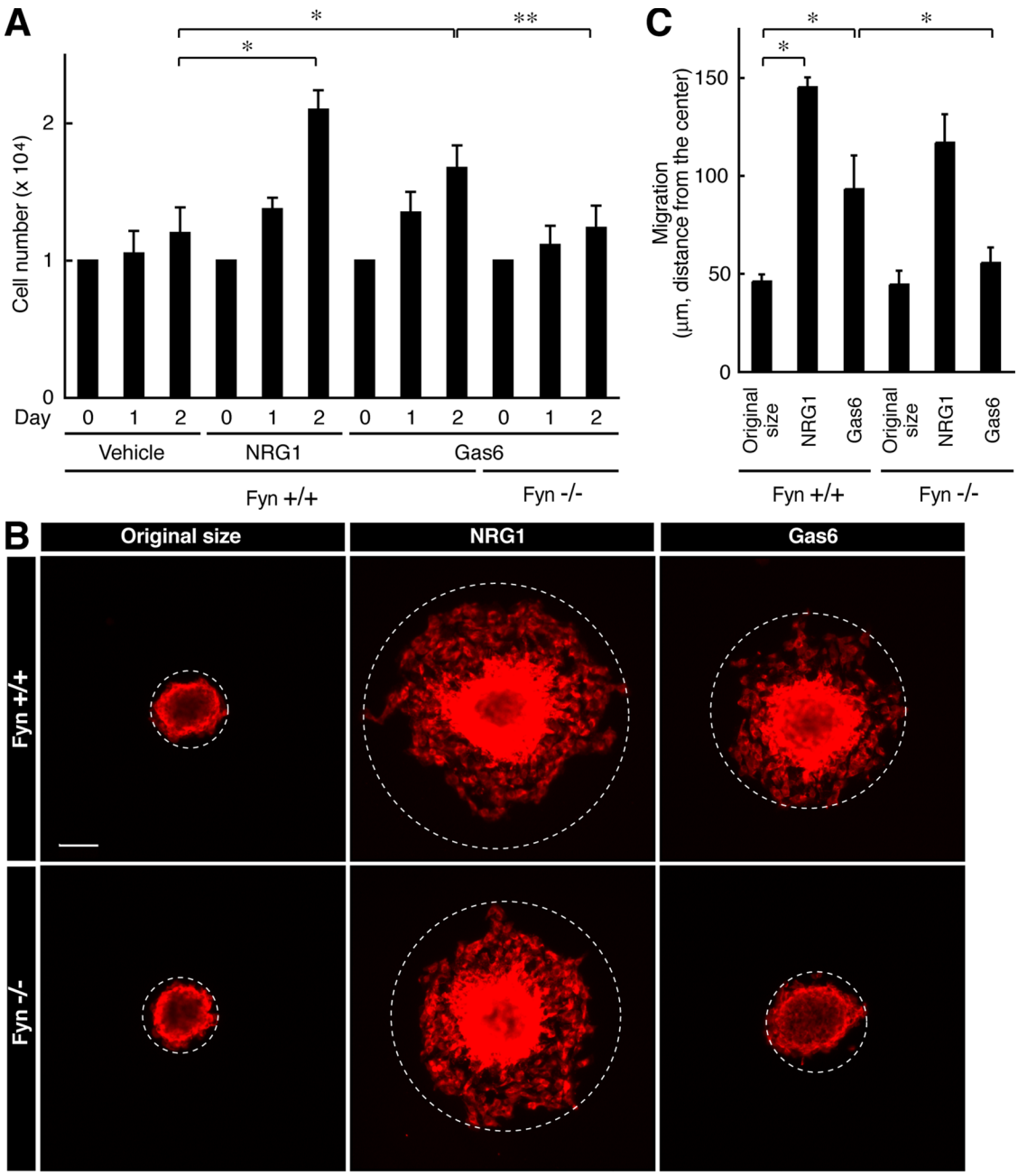

FIGURE 7: Deletion of Fyn inhibits Gas6-stimulated Schwann cell proliferation and migration. (A) Fyn$^{+/+}$ or Fyn$^{-/-}$ Schwann cells were cultured for 1 or 2 d in normal medium with or without Gas6 (*$p < 0.01$; **$p < 0.025$; $n = 4$). (B, C) Reaggregated Fyn$^{+/+}$ or Fyn$^{-/-}$ Schwann cells were allowed to migrate outward for 6 h in normal medium with or without Gas6 and stained with an antibody against S100β. The dotted circles indicate the maximum peripheries of Schwann cells migrating from the reaggregates (*$p < 0.01$; $n = 4$). Scale bar, 50 μm.

regeneration by controlling the receptor and the intracellular partner.

MATERIALS AND METHODS

Antibodies

The following antibodies were purchased: rabbit monoclonal anti-Tyro3 (5585S), rabbit monoclonal anti–neuronal marker GAP43 (8945S), rabbit monoclonal anti–68-kDa neurofilament NF68 (2835S), rabbit polyclonal anti-(pY527)Src (corresponding to pY531 in Fyn), and rabbit monoclonal anti–apoptotic marker active, cleaved caspase-3 (9579S) from Cell Signaling Technology (Danvers, MA); mouse monoclonal neuronal axon marker anti–βIII tubulin (MAB1195) from R&D Systems (Minneapolis, MN); mouse monoclonal anti-Fyn (05-436) and mouse monoclonal anti-(pS473) Akt (05-1003) from Merck-Millipore (Billerica, MA); rabbit polyclonal anti-Fyn (HPA023887) from Atlas Antibodies (Stockholm, Sweden); rabbit polyclonal anti–proliferating cell nuclear marker Ki67 (A0047) from Agilent Technology (Santa Clara, CA); mouse monoclonal anti-(pY416)Src (corresponding to pY420 in Fyn; sc-81521), mouse monoclonal anti-Akt1 (sc-5298), rabbit polyclonal anti-Oct6 (also called Scip; sc-133865), and rabbit polyclonal anti-Krox20 (also called Egr2; sc-20690) from Santa Cruz Biotechnology

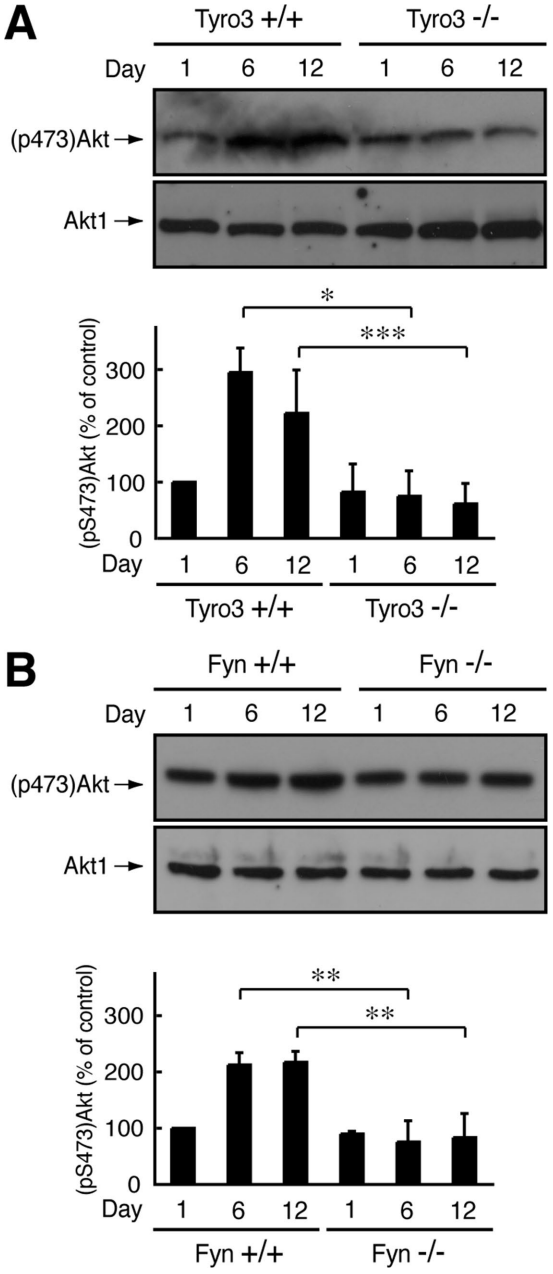

FIGURE 8: Effect of Tyro3 or Fyn knockout on Akt phosphorylation. (A, B) Tissue lysates from Tyro3 or Fyn ($^{+/+}$ or $^{-/-}$) mouse sciatic nerves were used for immunoblotting with an antibody against Akt1 or (pS473)Akt and the band intensities analyzed (*$p < 0.01$; **$p < 0.025$; ***$p < 0.05$; $n = 4$).

(Santa Cruz, CA); rabbit polyclonal anti-Tyro3 (ab109231) and mouse monoclonal anti-S100β (ab52642) from Abcam (Cambridge, United Kingdom); mouse monoclonal anti-MBP (SMI-94R-100) and monoclonal anti-GFAP (SMI-22R-100) from Covance (Princeton, NJ); anti-MPZ (also called P0) from MBL (Nagoya, Japan; rabbit polyclonal PD046) and Abnova (Taipei, Taiwan; goat polyclonal, PAB7332); mouse monoclonal anti–pan-sodium channel (K58/35) from Sigma-Aldrich (St. Louis, MO); mouse monoclonal anti-Rac1 (610652), mouse monoclonal anti-Cdc42 (610928), and mouse monoclonal anti–β-actin (612656) from Becton Dickinson (Franklin Lakes, NJ); mouse monoclonal anti–V5-epitope-tag (04434-94) from Nacalai Tesque (Kyoto, Japan); peroxidase-conjugated secondary antibodies from GE Healthcare (Fairfield, CT) and Nacalai Tesque; and fluorescence-labeled secondary antibodies from Life Technologies (Carlsbad, CA) and Wako Chemicals (Osaka, Japan).

Primers

The following primers were used in this study: 5′-ATGGCGCTGAGGCGGAGC-3′ (sense) and 5′-TGGGTCCTCTCCACCAGAAAATGGTTAC-3′ (antisense) for Tyro3; 5′-ATGGGCAGGGTCCCGCTG-3′ (sense) and 5′-GCATCTTGAAGCCAGAGCAGGGTC-3′ (antisense) for Axl; and 5′-ATGGTTCTGGCCCCACTACTGCT-3′ (sense) and 5′-GACCCATTGTCTGAGCGCTGCA-3′ (antisense) for Mertk. The control primers for β-actin were 5′-ATGGATGACGATATCGCTGCGCTC-3′ (sense) and 5′-CTAGAAGCATTTGCGGTGCACGATG-3′ (antisense). DNA primers were synthesized using the DNA synthesis service of Fasmac (Kanagawa, Japan).

Reverse transcription-PCR

Total RNA was extracted using TRIzol reagent (Life Technologies). Subsequently cDNAs were prepared from 1 μg of total RNA using Superscript reverse transcriptase (Life Technologies) according to the manufacturer's instructions. PCR amplification was performed using ExTaq DNA polymerase (Takara Bio, Kyoto, Japan) with 35 cycles, each consisting of denaturation at 94°C for 1 min, annealing at 61°C for 1 min, and extension at 72°C for 1 min.

Knockout mice

Tyro3-knockout mice (Stock number 007937) and Fyn-knockout mice (Stock number 002385) were obtained from the Jackson Laboratory (Hancock, ME; Stein *et al.*, 1992; Lu *et al.*, 1999). Heterozygous offspring were mated with wild-type C57BL/6JJms mice, and the mutations were propagated in this strain for an additional five generations before it was crossed to produce experimental homozygotes. Genomic PCR was performed to identify respective knockout alleles according to the Jackson Laboratory's standard protocol. Male mice were used for experiments when gender was distinguishable. Knockout mice are fertile under experimental breeding conditions and apparently normal.

Primary cell cultures

Primary DRG neurons and Schwann cells were collected from DRG of male or female mice on embryonic day 12.5 (Ratner *et al.*, 2006; Miyamoto *et al.*, 2008, 2012, 2013). In brief, DRG neurons were purified by culturing on collagen type I–coated dishes or wells in DMEM-GlutaMAX I (Life Technologies) containing 10% fetal bovine serum (FBS), 100 ng/ml nerve growth factor (NGF; AbD Serotec, Kidlington, United Kingdom), 8 μM fluorodeoxyuridine (Sigma-Aldrich), and 4 μM uridine (Sigma-Aldrich) in 95% humidified air/5% CO_2 at 37°C. After three cycles of antimitotic reagent administration over ~2 wk, purified DRG neurons were cultured in DMEM-GlutaMAX I containing 10% FBS and 50 ng/ml NGF. Schwann cells were isolated as Schwann cell precursors and cultured on collagen type I–coated dishes or wells in DMEM-GlutaMAX I containing 10% FBS and 100 ng/ml NGF at 37°C in 95% humidified air/5% CO_2. After 4 or 5 d, Schwann cells were detached from the dishes using 0.05% trypsin solution (Life Technologies) and cultured in normal growth medium (DMEM containing 5% FBS, B27 [Life Technologies], N2 [Life Technologies], and 2 μM forscolin [Nacalai Tesque]) in the presence or absence of 20 ng/ml of neuregulin-1 (NRG1; R&D Systems) or Gas6 (R&D Systems; Miyamoto *et al.*, 2012; Yamauchi *et al.*, 2012). Under these experimental conditions, trypan blue–incorporating cells

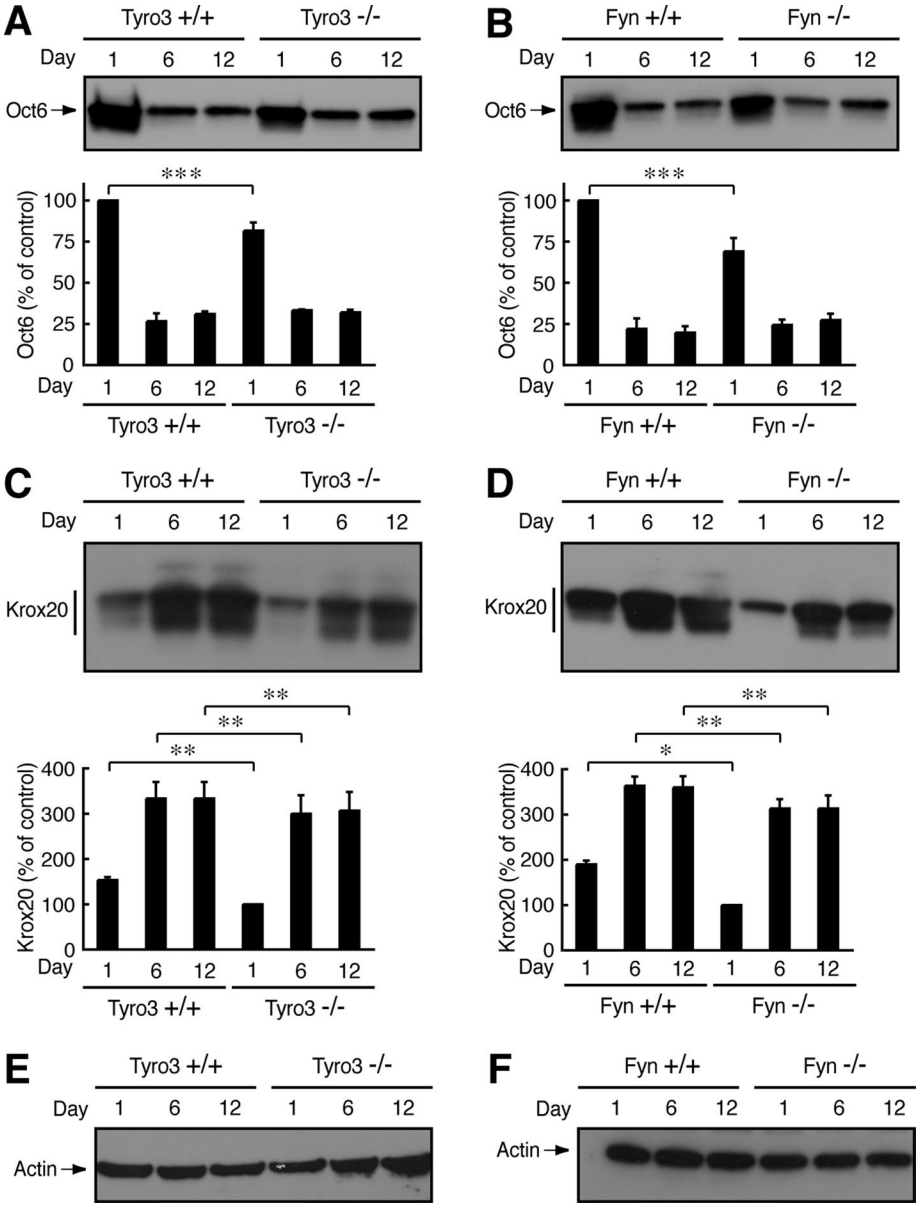

FIGURE 9: Effect of Tyro3 or Fyn knockout on Oct6 or Krox20 expression. (A, B) Tissue lysates from Tyro3 or Fyn ($^{+/+}$ or $^{-/-}$) mouse sciatic nerves were used for immunoblotting with an antibody against Oct6 and the band intensities analyzed (***p 0.05; $n = 3$). (C, D) Tissue lysates from Tyro3 or Fyn ($^{+/+}$ or $^{-/-}$) mouse sciatic nerves used for immunoblotting with an antibody against Krox20 (*p 0.01; **$p < 0.025$; n = 3). (E, F) Representative actin immunoblots in Tyro3 or Fyn ($^{+/+}$ or $^{-/-}$) nerves.

were <5%. Viable cells were counted using a hemocytometer (Life Technologies).

Migration assay

Cell migration assays were performed using Schwann cell reaggregates (Miyamoto *et al.*, 2012). The reaggregates were placed on dishes or in wells coated with collagen type I and allowed to migrate for 6 h. Maximal migration distances from the center of each reaggregate were measured.

Immunofluorescence

Cells on dishes or wells were fixed in phosphate-buffered saline (PBS) containing 4% paraformaldehyde and permeabilized using PBS containing 0.1% Tween-20. Permeabilized cells were blocked with Blocking One reagent (Nacalai Tesque); subsequently they were incubated with primary antibodies and then with fluorescence-labeled secondary antibodies. Thereafter the cells were mounted using Vectashield reagent (Vector Laboratories, Burlingame, CA) for microscopic observation. Fluorescence images were captured using a DMI4000 microscope system (Leica, Wetzlar, Germany) and analyzed using AF6000 software (software attached to DMI4000; Leica) or captured using an IX71 microscope system (Olympus, Tokyo, Japan) and analyzed using IX2-BSW software (software attached to IX71; Olympus).

In vitro myelination

Dissociated explants were established from male or female mice on embryonic day 12.5 (Yamauchi *et al.*, 2012). In brief, DRG were collected and dissociated using 0.25% trypsin and trituration. The cells were dispersed and plated onto collagen type I–coated coverslips (3×10^5 cells/coverslip). The dissociated explants were maintained in MEM containing 10% FBS and 100 ng/ml NGF. Axonal processes and endogenous Schwann cells were allowed to grow and establish for 5 d. Myelination was induced using 50 μg/ml ascorbic acid. The culture medium was changed every 2 or 3 d, and cultures were maintained for an additional 2 wk. Myelin segments, which were stained with an anti-MBP antibody, were considered those with a maximum fluorescence value of >2500 in the line profile scan program (Leica AF6000; Yamauchi *et al.*, 2010). They were counted in randomly selected 200-μm-square fields in more than three independent coverslips.

Plasmids

Human Tyro3 cDNA was obtained from the Kazusa DNA Research Institute (Chiba, Japan). The PCR-isolated intracellular kinase domain (amino acids 451–890) was ligated into the mammalian expression vector pCMV5 harboring the myc-epitope tag at the N-terminal position. The coding region of the pCMV5-V5-epitope–tagged isolated Fyn kinase (active Fyn) domain plasmid was inserted into mouse GFAP promoter-driven transgene expression plasmid (Yamauchi *et al.*, 2012). The active Fyn construct was originally provided from T. Yamamoto (University of Tokyo, Tokyo, Japan, and Okinawa Institute of Science and Technology, Onna, Okinawa, Japan). The mouse GFAP promoter plasmid was originally purchased from InvivoGen (San Diego, CA). In the PNS, the GFAP promoter is specifically active in Schwann cells, especially in the initiation of myelination (Mirsky *et al.*, 2008; Yamauchi *et al.*, 2012). The pET42a-active, GTP-bound Rac1, and Cdc42-binding domain (CRIB) plasmid was constructed as previously described (Miyamoto *et al.*, 2013). All DNA sequences were confirmed using the DNA sequence service of Fasmac.

Cell line culture and transfection

Rat immortalized RT4-D6P2T Schwann cells (EC93011415-F0) were obtained from DS Pharma Biomedical (Osaka, Japan) and cultured on dishes in DMEM containing 10% FBS, 50 U/ml penicillin, and 50 µg/ml streptomycin. The cells were transfected using Lipofectamine LTX-Plus reagent (Life Technologies) according to the manufacturer's instructions. Transfection efficiency with the control fluorescence protein–encoding plasmid was ~90%.

Identification of Tyro3's intracellular domain–interacting protein Fyn

RT4-D6P2T cells (1×10^8 cells) were transiently transfected with the plasmid encoding the myc-tagged intracellular domain of Tyro3 or with the control vector and lysed in lysis buffer A (50 mM 4-(2-hydroxyethyl)-1-piperazineethanesulfonic acid–NaOH, pH 7.5, 20 mM $MgCl_2$, 150 mM NaCl, 1 mM phenylmethane sulfonylfluoride, 1 µg/ml leupeptin, 1 mM EDTA, 1 mM Na_3VO_4, and 10 mM NaF) containing 0.5% NP-40 at 4°C (Yamauchi *et al.*, 2012; Miyamoto *et al.*, 2013). Protein complexes containing the intracellular domain were isolated from clear, centrifuged supernatants using the myc-tag protein mild purification kit (MBL) according to the manufacturer's instructions. Lysis buffer A containing 0.5% NP-40, 1.5 M NaCl, and 75 mM EDTA was used for the final elution. Diluted fractions containing the complexes were dialyzed using lysis buffer A containing 0.5% NP-40 and filtered through a 30,000–molecular weight cutoff membrane (Merck-Millipore). Samples were electrophoresed using SDS–PAGE and visualized with a silver staining kit (Nacalai Tesque). Protein bands were excised, enzymatically digested in gels, and analyzed by the proteome service of Cosmo Bio (Tokyo, Japan) using an Ettan MALDI-ToF Pro mass spectrometer (GE Healthcare) and Mascot database (Matrix Science, Boston, MA).

Generation of active Fyn transgenic mice

A DNA fragment (~4.5 kb) containing the SV40 enhancer, mouse GFAP promoter specific for Schwann cells in the PNS, V5-epitope–tagged active Fyn, and artificial intron, human chorionic gonadotropin polyA units (Yamauchi *et al.*, 2012) was digested from the vector backbone (~3.5 kb) with *Nco*I, purified, and injected into fertilized BDF1 oocytes. Transgenic founder mice and established transgenic mice were routinely identified by tail DNA genomic PCR (KAPA Biosystems, Wilmington, MA) with the specific primer pair 5′-CCGGAATTCGAATATTAGCTAGGAGTTTCAGAAAGGGGGCCTG-3′ and 5′-CCGGAATTCACTAGTGGGACTATGGTTGCTGACTAATTGAGATGC-3′ (Yamauchi *et al.*, 2012). PCR was performed in 35 cycles, each consisting of denaturation at 94°C for 0.5 min, annealing at 65°C for 0.5 min, and extension at 0.5°C for 1 min. The transgenic allele indicates 322 bases (Yamauchi *et al.*, 2012). Transgenic founders were mated to wild-type C57BL/6JJms mice. The littermates were mated to Tyro3-knockout mice, generating active Fyn-transgenic Tyro3-knockout mice and experimental controls. These mice were of the C57BL/6JJms- and BDF1-mixed background. The transgene was maintained until at least three generations.

Immunoprecipitation an immunoblotting

Tissues or cells were lysed in lysis buffer A containing 0.5% NP-40 or 0.5% NP-40, 1% 3-[(3-cholamidopropyl)dimethylammonio]-1-propanesulfonate, and 0.3% SDS at 4°C (Yamauchi *et al.*, 2012; Miyamoto *et al.*, 2013). Clear, centrifuged supernatants were examined by immunoprecipitation using the ImmunoCruz kit (Santa Cruz Biotechnology) according to the manufacturer's instructions. Immunoprecipitates or clear, centrifuged supernatants were boiled in the sample buffer (50 mM Tris-HCl, pH 6.8, 2% SDS, 30 mM dithiothreitol, 10% glycerol, and 0.01% bromophenol blue) and were applied to SDS–PAGE. The separated proteins were transferred onto polyvinylidene fluoride membranes, blocked with Blocking One reagent, and immunoblotted with primary antibodies, followed by a peroxidase-conjugated secondary antibody. Bound antibodies were detected using the chemiluminescence method (GE Healthcare and Wako Chemicals). The scanned protein bands were densitometrically analyzed using UN-SCAN-IT software.

Detection of active, GTP-bound Rho GTPases Rac1 and Cdc42

In brief, clear, centrifuged cell lysates were mixed with a recombinant glutathione *S*-transferase–tagged active Rac1 and Cdc42-binding CRIB from *Escherichia coli*, collected using a glutathione-conjugated resin, and immunoblotted using an antibody against Rac1 or Cdc42 (Miyamoto *et al.*, 2013). Rac1 and Cdc42 activities are essential for determining a neuronal morphology (Arimura and Kaibuchi, 2007; Hall and Lalli, 2010).

Immunohistochemistry

Tissues were perfused first with PBS and then with PBS containing 4% paraformaldehyde. For sodium channel staining, paraformaldehyde-fixed nerves were further teased using tweezers for rodent dissection (Terada *et al.*, 2013). The length between sodium channel–positive nodes was considered as that of the internode. Subsequently the tissues were postfixed with 4% paraformaldehyde, which was then replaced by 20% sucrose, and the tissues were embedded in Tissue-Tek reagent (Sakura Finetechnical, Tokyo, Japan). Microtome sections on glass slides were blocked using Blocking One reagent; subsequently they were incubated with primary antibodies and then with fluorescence-labeled secondary antibodies (Yamauchi *et al.*, 2012; Torii *et al.*, 2013). Glass slides were mounted using Vectashield reagent. Fluorescent images were captured using a DM2500 microscope system (Leica) and analyzed with LAS software (software attached to DMI2500; Leica) or captured with a BX51 microscope system (Olympus) and analyzed with DP2-BSW software (software attached to BX51; Olympus).

Electron microscopy

Tissues were fixed with 2% paraformaldehyde and 2% glutaraldehyde in 0.1% cacodylate buffer. They were then contrasted with 2% osmium tetroxide, dehydrated with an ethanol gradient, and treated with propylene oxide. Finally, the samples were infiltrated and embedded in pure epoxy resin. Ultrathin sections were stained with uranyl acetate and lead staining solution (Yamauchi *et al.*, 2012; Torii *et al.*, 2013). Images were taken using a JEM-1200EX electron microscope system (JOEL, Tokyo, Japan).

Measurement of nerve conduction velocity in the sciatic nerve

Anesthetized mice were placed on the heating pad. To stimulate nerve, stimulating electrodes (electrodes 45244 and 45157; GE Yokokawa-medicals, Tokyo, Japan) were placed above the left ankle and the left sciatic notch. Recording electrodes (electrodes 45244 and 45157) were placed in the footpad. Evoked compound muscle action potentials were obtained using an electromyography device (SEN-3301 system; Nihon Kohden, Tokyo, Japan), according to the protocol of the Nissei Bilis Research Center (Shiga, Japan). Distance between the two sites of stimulating electrodes was used to calculate conduction velocity. Average values of three experiments per mouse were considered as the respective nerve

conduction velocities. The experiments used 10 knockout mice and 10 controls.

Statistical analysis

Data are presented as mean ± SD from independent experiments. Intergroup comparisons were performed using Student's *t* test, and differences were considered significant when $*p < 0.01$, $**p < 0.025$, and $***p < 0.05$.

Animal studies

Genetically modified/unmodified mice were maintained in accordance with a protocol approved by the Japanese National Research Institute for Child Health and Development Animal Care Committee. Mice were monitored by the Laboratory Animal Facility of the Japanese National Research Institute for Child Health and Development. Gene recombinations were maintained in accordance with a protocol s approved by the Japanese National Research Institute for Child Health and Development Gene Recombination Committee and monitored by the Gene Recombination Committee.

ACKNOWLEDGMENTS

We thank K. Ikenaka, Y. Matsubara, H. Saito, and A. Umezawa for helpful discussions and acknowledge H. Sakonjo and T. Amano for measuring the nerve conduction velocity. We also thank C. Rowthorn and W. Fumanski for reading the manuscript. This work was supported by Grants-in-Aid for Young Scientist Research B, Scientific Research C, Scientific Research B, and Scientific Research on Innovative Areas (Glial assembly: a new regulatory machinery of brain function and disorders) from the Japanese Ministry of Education, Culture, Sports, Science, and Technology. This work was also supported by Grants-in-Aid for Scientific Research from the Japanese Ministry of Health, Labor, and Welfare and partially by the Takeda Foundation.

REFERENCES

Arimura N, Kaibuchi K (2007). Neuronal polarity: from extracellular signals to intracellular mechanisms. Nat Rev Neurosci 8, 194–205.

Binder MD, Cate HS, Prieto AL, Kemper D, Butzkueven H, Gresle MM, Cipriani T, Jokubaitis VG, Carmeliet P, Kilpatrick TJ (2008). Gas6 deficiency increases oligodendrocyte loss and microglial activation in response to cuprizone-induced demyelination. J Neurosci 28, 5195–5206.

Binder MD, Kilpatrick TJ (2009). TAM receptor signalling and demyelination. Neurosignals 17, 277–287.

Binder MD, Xiao J, Kemper D, Ma GZ, Murray SS, Kilpatrick TJ (2011). Gas6 increases myelination by oligodendrocytes and its deficiency delays recovery following cuprizone-induced demyelination. PLoS One 6, e17727.

Bunge RP (1993). Expanding roles for the Schwann cell: ensheathment, myelination, trophism and regeneration. Curr Opin Neurobiol 3, 805–809.

Chan JR, Cosgaya JM, Wu YJ, Shooter EM (2001). Neurotrophins are key mediators of the myelination program in the peripheral nervous system. Proc Natl Acad Sci USA 98, 14661–14668.

Cosgaya JM, Chan JR, Shooter EM (2002). The neurotrophin receptor p75NTR as a positive modulator of myelination. Science 298, 1245–1248.

Fritsch R, Downward J (2013). SnapShot: class I PI3K isoform signaling. Cell 154, 940.

Godowski PJ, Mark MR, Chen J, Sadick MD, Raab H, Hammonds RG (1995). Reevaluation of the roles of protein S and Gas6 as ligands for the receptor tyrosine kinase Rse/Tyro3. Cell 82, 355–358.

Hai M, Muja N, De Vries GH, Quarles RH, Patel PI (2002). Comparative analysis of Schwann cell lines as model systems for myelin gene transcription studies. J Neurosci Res 69, 497–508.

Hall A, Lalli G (2010). Rho and Ras GTPases in axon growth, guidance, and branching. Cold Spring Harb Perspect Biol 2, a001818.

Hossain S, Fragoso G, Mushynski WE, Almazan G (2010). Regulation of peripheral myelination by Src-like kinases. Exp Neurol 226, 47–57.

Hunter T (2009). Tyrosine phosphorylation: thirty years and counting. Curr Opin Cell Biol 21, 140–146.

Klein C, Kramer EM, Cardine AM, Schraven B, Brandt R, Trotter J (2002). Process outgrowth of oligodendrocytes is promoted by interaction of fyn kinase with the cytoskeletal protein tau. J Neurosci 22, 698–707.

Krishnan A (2013). Neuregulin-1 type I: a hidden power within Schwann cells for triggering peripheral nerve remyelination. Sci Signal 6, jc1.

Lemke G (2001). Glial control of neuronal development. Annu Rev Neurosci 24, 87–105.

Lemke G, Rothlin CV (2010). Immunobiology of the TAM receptors. Nat Rev Immunol 8, 327–336.

Li R, Chen J, Hammonds G, Phillips H, Armanini M, Wood P, Bunge R, Godowski PJ, Sliwkowski MX, Mather JP (1996). Identification of Gas6 as a growth factor for human Schwann cells. J Neurosci 16, 2012–2019.

Lu Q, Gore M, Zhang Q, Camenisch T, Boast S, Casagranda F, Lai C, Skinner MK, Klein R, Matsushima GK, *et al*. (1999). Tyro-3 family receptors are essential regulators of mammalian spermatogenesis. Nature 398, 723–728.

Macklin WB (2010). The myelin brake: when enough is enough. Sci Signal 3, pe32.

Mirsky R, Woodhoo A, Parkinson DB, Arthur-Farraj P, Bhaskaran A, Jessen KR (2008). Novel signals controlling embryonic Schwann cell development, myelination and dedifferentiation. J Peripher Nerv Syst 13, 122–135.

Miyamoto Y, Torii T, Yamamori N, Eguchi T, Nagao M, Nakamura K, Tanoue A, Yamauchi J (2012). Paxillin is the target of c-Jun N-terminal kinase in Schwann cells and regulates migration. Cell Signal 24, 2061–2069.

Miyamoto Y, Torii T, Yamamori N, Ogata T, Tanoue A, Yamauchi J (2013). Akt and PP2A reciprocally regulate the guanine nucleotide exchange factor Dock6 to control axon growth of sensory neurons. Sci Signal 6, ra15.

Miyamoto Y, Yamauchi J (2014). Recent insights into molecular mechanisms that control growth factor receptor-mediated Schwann cell morphological changes during development. In: Schwann Cell Development and Pathology, ed. K Sango and J Yamauchi, New York: Springer, 5–27.

Miyamoto Y, Yamauchi J, Tanoue A (2008). Cdk5 phosphorylation of WAVE2 regulates oligodendrocyte precursor cell migration through nonreceptor tyrosine kinase Fyn. J Neurosci 28, 8326–8337.

Monje PV, Rendon S, Athauda G, Bates M, Wood PM, Bunge MB (2009). Non-antagonistic relationship between mitogenic factors and cAMP in adult Schwann cell re-differentiation. Glia 57, 947–961.

Nave KA, Salzer JL (2006). Axonal regulation of myelination by neuregulin 1. Curr Opin Neurobiol 16, 492–500.

Ness JK, Snyder KM, Tapinos N (2013). Lck tyrosine kinase mediates b1-integrin signalling to regulate Schwann cell migration and myelination. Nat Commun 4, 1912.

Newbern J, Birchmeier C (2010). Nrg1/ErbB signaling networks in Schwann cell development and myelination. Semin Cell Dev Biol 21, 922–928.

Novak N, Bar V, Sabanay H, Frechter S, Jaegle M, Snapper SB, Meijer D, Peles E (2011). J Cell Biol 192, 243–250.

Ogata T, Iijima S, Hoshikawa S, Miura T, Yamamoto S, Oda H, Nakamura K, Tanaka S (2004). Opposing extracellular signal-regulated kinase and Akt pathways control Schwann cell myelination. J Neurosci 24, 6724–6732.

Pereira JA, Lebrun-Julien F, Suter U (2012). Molecular mechanisms regulating myelination in the peripheral nervous system. Trends Neurosci 35, 123–134.

Ratner N, Williams JP, Kordich JJ, Kim HA (2006). Schwann cell preparation from single mouse embryos: analyses of neurofibromin function in Schwann cells. Methods Enzymol 407, 22–33.

Sperber BR, Boyle-Walsh EA, Engleka MJ, Gadue P, Peterson AC, Stein PL, Scherer SS, McMorris FA (2001). A unique role for Fyn in CNS myelination. J Neurosci 21, 2039–2047.

Spiegel I, Adamsky K, Eshed Y, Milo R, Sabanay H, Sarig-Nadir O, Horresh I, Scherer SS, Rasband MN, Peles E (2007). A central role for Necl4 (SynCAM4) in Schwann cell-axon interaction and myelination. Nat Neurosci 10, 861–869.

Stein PL, Lee HM, Rich S, Soriano P (1992). p59fyn mutant mice display differential signaling in thymocytes and peripheral T cells. Cell 70, 741–750.

Stitt TN, Conn G, Gore M, Lai C, Bruno J, Radziejewski C, Mattsson K, Fisher J, Gies DR, Jones PF, *et al*. (1995). The anticoagulation factor protein S and its relative, Gas6, are ligands for the Tyro3/Axl family of receptor tyrosine kinases. Cell 80, 661–670.

Taniguchi S, Liu H, Nakazawa T, Yokoyama K, Tezuka T, Yamamoto T (2003). p250GAP, a neural RhoGAP protein, is associated with and phosphorylated by Fyn. Biochem Biophys Res Commun 306, 151–155.

Taveggia C, Feltri ML, Wrabetz L (2010). Signals to promote myelin formation and repair. Nat Rev Neurol 6, 276–287.
Terada N, Saitoh Y, Ohno N, Komada M, Yamauchi J, Ohno S (2013). Involvement of Src in the membrane skeletal complex, MPP6-4.1G, in Schmidt-Lanterman incisures of mouse myelinated nerve fibers in PNS. Histochem Cell Biol 140, 213–222.
Torii T, Miyamoto Y, Onami N, Tsumura H, Nemoto N, Kawahara K, Kato M, Kotera J, Nakamura K, Tanoue A, Yamauchi J (2013). In vivo expression of the Arf6 guanine-nucleotide exchange factor cytohesin-1 in mice exhibits enhanced myelin thickness in nerves. J Mol Neurosci 51, 522–531.
Toshima J, Ohashi K, Iwashita S, Mizuno K (1995). Autophosphorylation activity and association with Src family kinase of Sky receptor tyrosine kinase. Biochem Biophys Res Commun 209, 656–663.
Tsiperson V, Li X, Schwartz GJ, Raine CS, Shafit-Zagardo B (2010). GAS6 enhances repair following cuprizone-induced demyelination. PLoS One 5, e15748.
Umemori H, Sato S, Yagi T, Aizawa S, Yamamoto T (1994). Initial events of myelination involve Fyn tyrosine kinase signalling. Nature 367, 572–576.
Wolf RM, Wilkes JJ, Chao MV, Resh MD (2001). Tyrosine phosphorylation of p190 RhoGAP by Fyn regulates oligodendrocyte differentiation. J Neurobiol 49, 62–78.
Yamauchi J, Miyamoto Y, Torii T, Takashima S, Kondo K, Kawahara K, Nemoto N, Chan JR, Tsujimoto G, Tanoue A (2012). Phosphorylation of cytohesin-1 by Fyn is required for initiation of myelination and the extent of myelination during development. Sci Signal 5, ra69.
Yamauchi J, Torii T, Kusakawa S, Sanbe A, Nakamura K, Takashima S, Hamasaki H, Kawaguchi S, Miyamoto Y, Tanoue A (2010). The mood stabilizer valproic acid improves defective neurite formation caused by Charcot-Marie-Tooth disease-associated mutant Rab7 through the JNK signaling pathway. J Neurosci Res 88, 3189–3197.